Structural Measurements on the Liquid-Crystal Analog of the Abrikosov Phase

G. Srajer, R. Pindak, M. A. Waugh, and J. W. Goodby[a]
AT&T Bell Laboratories, Murray Hill, New Jersey 07974

J. S. Patel
Bellcore, Redbank, New Jersey 07701
(Received 15 November 1989)

High-resolution x-ray and optical studies were performed on oriented samples of the recently discovered smectic-A^* phase. We confirm that this phase exhibits smectic-A layers as well as a macroscopic helical structure with the helical axis parallel to the layer planes. Furthermore, we demonstrate that the observed scattering can be explained by a cylindrical structure factor that is, within our instrumental resolution, a δ function in the radial direction and a Gaussian in the transverse direction as predicted by Renn and Lubensky for the "twist-grain-boundary" phase.

PACS numbers: 61.10.Lx, 61.30.Eb, 78.20.Dj

The analogy between a superconductor and a smectic-A (Sm-A) liquid-crystal phase was first recognized by de Gennes.[1] The Sm-A phase is a layered phase in which the average molecular orientation, called the "director," is normal to the plane of the layers. According to the analogy, the application of a twist or bend distortion to a Sm-A liquid crystal is analogous to the application of a magnetic field to a superconductor. In the latter case, the magnetic field is either expelled (type-I behavior) or incorporated in a lattice of flux vortices referred to as the Abrikosov flux lattice[2] (type-II behavior). Although it was recognized that, for an applied twist distortion, the liquid-crystal analog of the superconductor flux vortices were screw dislocations, it was not known *how* or *if* these screw dislocations would exhibit type-II behavior and form ordered arrays until two, *concurrent*, recent advances. On the theoretical front, Renn and Lubensky postulated[3] a specific model for the liquid-crystal analog of the type-II Abrikosov flux lattice. Their model consists of regularly spaced grain boundaries of screw dislocations which are parallel to each other within the grain boundary, but are rotated by a fixed angle with respect to screw dislocations in adjacent grain boundaries. They named the resultant phase a "twist-grain-boundary" (TGB) phase. On the experimental front, Goodby *et al.*[4] reported the discovery of a novel, smectic-A-like phase composed of chiral molecules in which the layers twist along an axis parallel to the layer planes, thus forming a macroscopic helical structure. They referred to this phase as a smectic A^*. Their initial optical, calorimetric, and x-ray investigations showed that the TGB phase of Renn and Lubensky was a feasible model for the smectic-A^* (A^*) phase.

In this Letter, we report the first detailed optical and high-resolution x-ray studies on well-aligned A^* samples. We make quantitative comparisons between the structural properties of the A^* phase and those predicted for the TGB phase. First, our optical measurements establish the existence of a macroscopic helical structure because aligned samples selectively reflect right circularly polarized light. Furthermore, we obtain the pitch of the helix as a function of temperature by measuring the wavelength dependence of the transmitted light. Second, using x-ray scattering we confirm that the orientation of the A^* layers is parallel to the pitch axis. Finally, we perform high-resolution x-ray scans and show that the scattering is what would be expected from an array of screw dislocations ordered as in the TGB phase.

To obtain an aligned sample, the internal surfaces of thin (~ 150 μm), flat pieces of glass were polymer coated and unidirectionally buffed.[5] This procedure promotes an alignment of the molecular director parallel to the glass plates which, in turn, means that the helical pitch axis is oriented perpendicularly to the boundaries. Several sample cells with thickness from 10 to 25 μm were assembled. The quality of the alignment was optically evaluated by rotating the cell between crossed polarizers. Excellent alignment, independent of thickness, was achieved in all samples. The liquid-crystal compound studied was the R-enantiomer of 1-methylheptyl 4'-[[(4"-tetradecyloxyphenyl)propioloyl]-oxy] biphenyl-4-carboxylate (+14P1M7). This compound is from the same homologous series originally studied by Goodby *et al.*[4] It exhibits a smectic-C^*-to-A^* transition at 90 °C followed by an A^*-to-isotropic transition at 94 °C. Goodby *et al.*[4] argue that this phase sequence enhances the likelihood of +14P1M7 satisfying the Ginzburg criteria[6] for type-II behavior since its twist penetration length (analogous to the London length) diverges at the A^*-to-C^* transition while its layer coherence length remains finite. This plausibility argument was subsequently further developed[7] and shown to be correct.

To demonstrate that the A^* phase forms a macroscopic helical structure, the wavelength dependence of the transmitted intensity of circularly polarized light was measured. The sample cell was placed in a hot stage

whose temperature was regulated to ± 10 mK. Light from a 75-W xenon arc lamp was first passed through a monochromator and appropriate filters then focused onto the sample. The range of incident wavelengths was varied between 500 and 1600 nm with a resolution of 2 nm full width at half maximum (FWHM). The transmitted intensity was detected by either a Si or Ge photodiode. The inset to Fig. 1 shows typical transmission spectra for right (solid line) and left (dashed line) circularly polarized light obtained using a 20-μm-thick sample of +14P1M7 at 92.8 °C. The spectra have been normalized to the source intensity and plotted as a ratio of the measured intensity to the corresponding intensity in a reference spectrum taken when the sample was heated to the isotropic phase. This latter procedure compensates for any wavelength dependence in the optical elements as well as in the spectral response of the photodiodes. As seen in the inset, the transmission spectra for right circularly polarized light can be characterized by a Bragg reflection band centered at λ_m with FWHM of $0.12\lambda_m$. Since the sample selectively reflects right circularly polarized light, this confirms that the A^* phase of

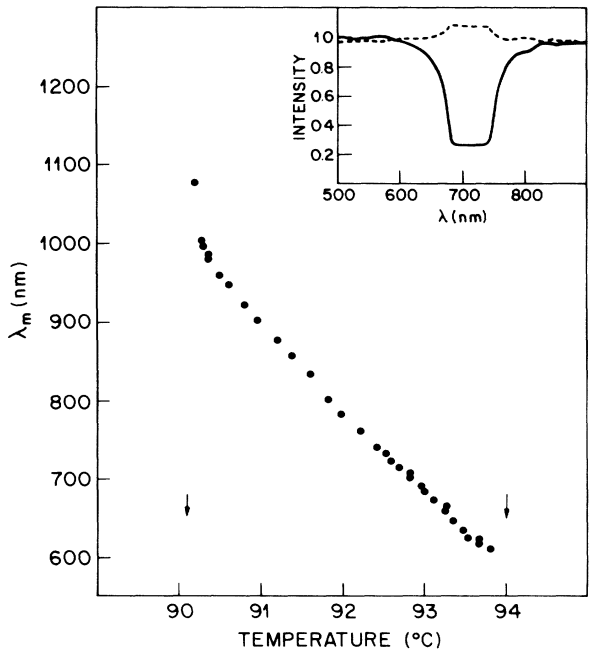

FIG. 1. Since the A^* phase of +14P1M7 Bragg reflects right circularly polarized light, there is a corresponding notch in the transmission spectrum centered at the wavelength λ_m. The temperature dependence of λ_m is shown. The arrow on the left indicates the transition temperature between the C^* and A^* phases, while the arrow on the right indicates the higher-temperature A^*-to-isotropic transition. Inset: Typical transmission spectra for right circularly polarized light (solid line) as well as left circularly polarized light (dashed line). The transmission notch for right circularly polarized light is evident.

+14P1M7 exhibits a right-hand helical structure.[8] The absolute value of the pitch, λ_0, of this helical structure is related to λ_m by $\lambda_m = \lambda_0 \bar{n}$, where $\bar{n} \approx 1.6$ is the average index of refraction of the A^* phase. In Fig. 1, λ_m is plotted as a function of temperature. Except for a small pretransitional increase near the C^*-to-A^* transition, λ_m increases linearly with decreasing temperature indicating a corresponding linear increase in the A^* pitch from 0.38 to 0.63 μm.

The next step was to probe the relative orientation of layers with respect to the pitch of the helix by x-ray scattering. The experiment was performed utilizing Cu $K\alpha$ radiation from an 18-kW rotating anode x-ray generator. A vertically bent pyrolytic graphite (002) crystal focused the x rays to a 0.5×2-mm^2 spot on the sample and the scattered radiation was analyzed by slits. The resultant instrumental resolution was 0.002° FWHM in the scan direction. The sample cell was placed in a two-stage oven which provided temperature stability of ± 10 mK.

The alignment procedure involved, first, setting the temperature of the oven so the sample was in the C^* phase where the smectic layers align in a well-characterized chevron structure.[9] Then, C^*-layer scattering peaks were used to determine the orientation of the normal to the glass plates of the sample cell, $\hat{\mathbf{n}}_G$. Subsequently, the sample was heated to the A^* phase and the momentum-transfer vector, $\mathbf{Q}_s$, set to a fixed value $|\mathbf{Q}_s| = 2\pi/d$, where d was the A^*-layer spacing. Referring to the lower inset to Fig. 2, we define a β scan as a rotation of the sample cell about an axis perpendicular to both $\hat{\mathbf{n}}_G$ and $\mathbf{Q}_s$ with $\beta = 0$ when $\hat{\mathbf{n}}_G \perp \mathbf{Q}_s$. Since $\hat{\mathbf{n}}_G$ coincides with the helical pitch axis, $\hat{\mathbf{P}}$, a β scan reveals the desired layer orientation. A typical β scan is shown in Fig. 2. Although the scattering peak is broad (its width is related to the width of the scattering peak in the $Q_\perp$ scan described below), it clearly has a peak at $\beta = 0$. This quantitatively confirms that the A^* layers are oriented parallel to the pitch axis as schematically illustrated in the upper inset to Fig. 2.

In the final section of the paper we present high-resolution x-ray measurements on the A^* phase. To compare these results with the x-ray scattering expected from the TGB phase, we first review the structure proposed by Renn and Lubensky for the TGB phase applied, specifically, to the material parameters of +14P1M7. We, then, review the x-ray scattering expected from such a structure and, lastly, make comparisons with the A^* measurements. Referring to the upper inset to Fig. 2, in the TGB model it is grain boundaries of parallel screw dislocations which rotate the "blocks" of smectic layers. If the screw dislocations within each grain boundary are separated by l_d, then the grain boundary rotates adjacent blocks of smectic layers by an angle $\Delta\Theta = d/l_d$. A second grain boundary, a distance l_b away, then rotates the next block through $\Delta\Theta$. This continues resulting in a

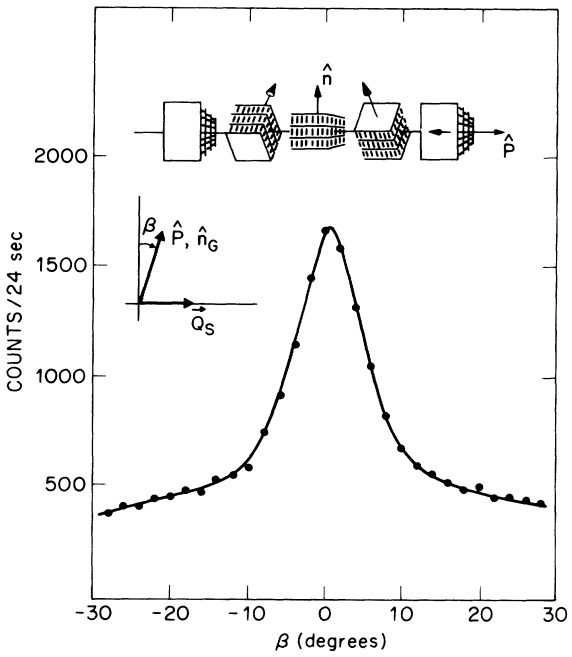

FIG. 2. Scattered intensity as a function of β, for fixed momentum transfer $|\mathbf{Q}_s|$. β is an angle between the normal to the glass plates, $\hat{\mathbf{n}}_G$, or, equivalently, the pitch direction and the momentum-transfer vector $\mathbf{Q}_s$ (lower inset). The solid line through the data points is only a guide to the eye. Upper inset: A schematic model of the A^* phase. $\hat{\mathbf{P}}$ is the pitch axis of the helix and $\hat{\mathbf{n}}$ is the molecular director oriented perpendicular to the smectic layers (only a half pitch is depicted). The "blocks" of smectic layers have an infinite extent in the direction transverse to the pitch axis.

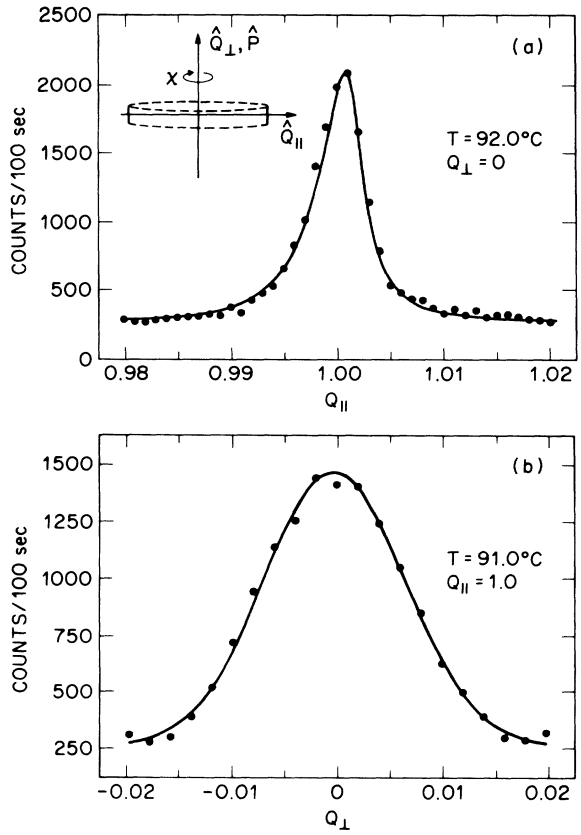

FIG. 3. (a) A $Q_\parallel$ scan taken at a temperature in the A^* phase. The solid line through the data points is a two-dimensional convolution of the $(Q_\parallel, Q_t)$ instrumental resolution with the predicted TGB cylindrical structure factor which is shown schematically in the inset. $Q_\parallel$ is in units of $2\pi/d = 0.146$ Å^{-1}. (b) A $Q_\perp$ scan ($Q_\parallel = 1$) taken at a temperature in the A^* phase. The solid line through the data points is a fit to a Gaussian. The resolution width for the $Q_\perp$ scan ($\Delta Q_\perp = 1.1 \times 10^{-5}$ Å^{-1}) was too small to illustrate. $Q_\perp$ is in units of 1.676 Å^{-1}.

macroscopic helical structure. The two lengths, l_b and l_d, which describe the spacing between screw dislocations, are related to the helical pitch by $l_b l_d = d\lambda_0/2\pi$. A reasonable[3] estimate of the spacing between screw dislocations can be obtained by taking $l_b = l_d = l$. Then, using average parameters measured for +14P1M7, we obtain $l = (d\lambda_0/2\pi)^{1/2} \approx 185$ Å and hence, $\Delta\Theta \approx 13°$ or there are 27 blocks per pitch.

It is easiest to reference the scattering Renn and Lubensky predict for the TGB phase to the scattering peaks from an aligned Sm-A sample. Taking $Q_\parallel$ and $Q_\perp$ as, respectively, the momentum transfer parallel and perpendicular to the molecular director, and Q_t as orthogonal to $Q_\parallel$ and $Q_\perp$, then the Sm-A layer peaks occur along the $Q_\parallel$ axis at $\pm Q_0 = 2\pi/d$, where d is the layer spacing. The helical rotation of the blocks of smectic layers turns the Sm-A scattering peaks into a ring of scattering in the $(Q_\parallel, Q_t)$ plane [inset to Fig. 3(a)]. Since the grain boundaries do not disrupt the smectic layering in the direction normal to the layers and layer fluctuations are not included in the TGB model, the structure factor in the $(Q_\parallel, Q_t)$ plane is a δ function along the radius Q_0. The grain boundaries do, however, disrupt the layering in a direction parallel to the smectic layers so the ring of scattering is broadened in the $Q_\perp$ direction into a cylinder of scattering whose height is described by a Gaussian of characteristic width $L = 2\pi/(\lambda_{c2} d)^{1/2}$, where λ_{c2} is the cholesteric pitch at the upper critical field. Since +14P1M7 does not contain a cholesteric phase, we estimate L by setting λ_{c2} equal to the pitch measured for +14P1M7 at the A^*-to-isotropic transition. In this way we obtain $L \approx 0.016$ Å^{-1}. Finally, we note that if $\Delta\Theta$ is a rational fraction of 2π, then the cylinder of scattering can develop further structure around its circumference.

To make a detailed comparison between the scattering from the A^* phase and the structure factor predicted for the TGB phase, high-resolution x-ray scans were performed on beam line X16B at the National Synchrotron Light Source. With the sample in a transmission geometry, the scattering is defined by the axes $Q_\parallel$, $Q_\perp$, and Q_t [inset to Fig. 3(a)]. The in-plane resolution of

the spectrometer, defined primarily by the monochromator and analyzer Ge(111) crystals, was $\Delta Q_{\parallel}=5.4\times10^{-4}$ Å^{-1} and $\Delta Q_{\perp}=1.1\times10^{-5}$ Å^{-1} (FWHM), while the resolution in the transverse direction, defined by 1-mm slits, was $\Delta Q_t=1.4\times10^{-2}$ Å^{-1} (FWHM). The x-ray beam, at the sample position, probed a 1-mm^2 area.

Two different types of scans, one along $Q_{\parallel}$ and the other along $Q_{\perp}$, are necessary to relate the scattering from the oriented A^* sample with the scattering cylinder of the TGB phase. A typical $Q_{\parallel}$ scan ($Q_{\perp}=0$) is shown in Fig. 3(a). The solid line is a fit of the data to a two-dimensional convolution in the $(Q_{\parallel},Q_t)$ plane of the instrumental resolution with the predicted radial TGB δ-function structure factor and a constant background term. It is evident that the structure factor correctly describes the data. The width of the peak is essentially determined by the $Q_{\parallel}$ instrumental resolution with a slight ($\sim$10%) asymmetric broadening arising since a radial $Q_{\parallel}$ scan through the cylinder of scattering will detect excess off-axis scattering on the low-Q side of the peak due to the finite Q_t resolution. The fact that a radial δ-function structure factor describes the A^* scattering within our instrumental resolution strongly supports the TGB model as the appropriate one and, moreover, enables us to set a *lower limit* to the A^*-layer correlations of 5000 Å. It is important to note that, as has been demonstrated[10] for the Sm-A phase using triple-reflection channel-cut crystals, layer fluctuations change the structure factor which describes the Sm-A scattering from a δ function into a structure factor $S(Q_{\parallel})\sim(Q_{\parallel}-Q_0)^{-2+\eta}$, with $\eta\sim0.2$–0.4. Although layer fluctuations are undoubtedly also present in the A^* phase, the subtle distinction between these two structure factors would not be observable using a single-face crystal analyzer,[10] and so we have used the δ-function structure factor as an approximation appropriate for our instrumental resolution.

The second type of scan was a $Q_{\perp}$ scan with $Q_{\parallel}=1.0$. This scan is shown in Fig. 3(b). The solid line is a fit of the data to a Gaussian line shape of characteristic width $L=0.033$ Å^{-1}. As previously discussed, both the Gaussian line shape and its width are in good agreement with the TGB model providing further support for its validity. It is important to note that the $Q_{\perp}$ instrumental resolution was a factor of 3000 narrower than the width of the $Q_{\parallel}$ scattering; hence, it was not necessary to include the $Q_{\perp}$ resolution in the analysis of the $Q_{\parallel}$ scan. Next, to estimate the degree of alignment of the pitch axis in our samples, several scans were done along $Q_{\parallel}$ with $Q_{\perp}=\pm0.01$. There was no observable shift in the $Q_{\parallel}$ peak position. This implies that the pitch axis was aligned to better than 1° within the 1-mm^2 area probed. We also performed χ scans to look for structure around the circumference of the cylinder of scattering; but, none was found. Finally, we repeated the $Q_{\parallel}$ and $Q_{\perp}$ scans at different temperatures throughout the A^* range. The $Q_{\parallel}$ line shape remained unchanged, while the $Q_{\perp}$ line shape sharpened by $\sim$11% with decreasing temperature. This is consistent with the fact that the number of screw dislocations decreases with decreasing temperature since the A^* pitch increases.

In summary, we have shown that when probed at optical ($\sim$5000 Å) and x-ray ($\sim$40 Å) length scales, the structural properties of the A^* phase of +14P1M7 agree in quantitative detail with those predicted by Renn and Lubensky for the TGB phase. It remains to probe the lattice of screw dislocations in the A^* phase directly at a length scale commensurate with their $\sim$185-Å lattice spacing. This length scale is accessible to small-angle x-ray scattering as well as electron microscopy on freeze-fracture preparations.[11] Experiments using both techniques are currently in progress.

We are grateful for helpful discussions with Scott Renn, Tom Lubensky, Denis McWaugh, Eric Isaacs, Steve Davey, and David Huse. Work at the National Synchrotron Light Source, Brookhaven National Laboratory, is supported by the U.S. Department of Energy under Contract No. DE-AC02-76CH00016.

[a]Current address: School of Chemistry, The University, Hull, HU6 7RX, England.

[1]P. G. de Gennes, Solid State Commun. **10**, 753 (1972).

[2]A. A. Abrikosov, Zh. Eksp. Teor. Fiz. **32**, 1442 (1957) [Sov. Phys. JETP **5**, 1174 (1957)].

[3]S. R. Renn and T. C. Lubensky, Phys. Rev. A **38**, 2132 (1988).

[4]J. W. Goodby, M. A. Waugh, S. M. Stein, E. Chin, R. Pindak, and J. S. Patel, Nature (London) **337**, 449 (1989); J. Am. Chem. Soc. **111**, 8119 (1989).

[5]J. Patel, T. M. Leslie, and J. W. Goodby, Ferroelectrics **57**, 137 (1984).

[6]See, for example, M. Tinkham, *Introduction to Superconductivity* (McGraw-Hill, New York, 1975).

[7]T. C. Lubensky and S. R. Renn, Phys. Rev. A (to be published).

[8]See, for example, P. G. de Gennes, *The Physics of Liquid Crystals* (Oxford Univ. Press, Oxford, 1975), p. 221.

[9]T. P. Rieker, N. A. Clark, G. S. Smith, D. S. Parmar, E. B. Sirota, and C. R. Safinya, Phys. Rev. Lett. **59**, 2658 (1987).

[10]J. Als-Nielsen, J. D. Litster, R. J. Birgeneau, M. Kaplan, C. R. Safinya, A. Lindegaard-Andersen, and S. Mathiesen, Phys. Rev. B **22**, 312 (1980).

[11]J. A. N. Zasadzinski (to be published).